

Incoherent topological defect recombination dynamics in TbTe_3

T. Mertelj¹, V. V. Kabanov¹, I. Fisher² and D. Mihailovic^{1,3}

¹*Complex Matter Department, Jozef Stefan Institute, Jamova 39, 1000 Ljubljana, Slovenia*

²*Stanford University, California, USA and*

³*CENN Nanocentre, Jamova 39, 1000 Ljubljana, Slovenia*

(Dated: August 7, 2012)

We study the incoherent recombination of topological defects created during a rapid quench of a charge-density-wave system through the electronic ordering transition. Using a specially devised 3-pulse femtosecond optical spectroscopy technique we follow the evolution of the order parameter over a wide range of timescales. By careful consideration of thermal processes we can clearly identify intrinsic topological defect annihilation processes on a timescale ~ 30 ps and find a signature of extrinsic defect-dominated relaxation dynamics occurring on longer timescales.

PACS numbers: 71.45.Lr, 78.47.jh, 63.20.kp

Topological defects are non-linear objects which can be created any time a symmetry-breaking transition occurs.[1–3] They are predicted theoretically as solutions to systems of nonlinear differential equations based on Ginzburg-Landau theory. They are of great fundamental importance in fields such as cosmology where they appear as strings and condensed matter physics where they appear in the form of vortices and domain walls. While a good understanding of static properties of topological defects (TD) has come from systems such as liquid crystals, the dynamics of TDs are much less understood. Electronic phase transitions in charge-density wave systems[4] are particularly interesting model systems for studying the general behavior of the dynamics of topological excitations. The collective excitations are not overdamped which allows the observation of both collective and quasi-particle (QP) excitations as they evolve through the transition. In particular, they can be used to investigate the dynamic behavior of topological excitations such as domain walls in real time using ultrafast laser techniques.

Recently, time-resolved experiments have shown that following a quench created by a strong laser pulse the order parameter (OP) oscillates coherently, revealing coherent TD dynamics.[5] Domain walls are created parallel to the crystal surface which can coherently annihilate on the timescale of a few picoseconds with the accompanying emission of collective modes which have been detected as modulations of reflectivity upon reaching the surface. In addition to coherent defect dynamics, incoherent topological defects created by the Kibble-Zurek mechanism[2] are also expected, but very little is known about the dynamics of incoherent TD dynamics in CDW systems, and in condensed matter systems in general.

In this paper we investigate the incoherent evolution of TDs using a specially devised 3-pulse femtosecond spectroscopy[5] technique which allows the direct background free observation of the evolution of the order parameter (OP) as a function of time through the electronic ordering transition. In a rapid quench experiment order emerges in different regions of the sample independently so multiple topological defects can be created. Their presence can be detected in the optical response as

a spatial inhomogeneity of the order parameter. The determination of incoherent TD dynamics is a challenging task, however. Because of thermal diffusion processes, which evolve on similar timescales as topological annihilation and also introduce temperature inhomogeneity, careful temperature calibration from independently measured frequencies is needed to accurately account for thermal effects. We deal with the problem by careful calibration of the transient effective temperatures, which enables us to unambiguously distinguish the incoherent dynamics from thermal diffusion effects.

In our experiments, we use a three pulse technique described in refs. [5, 6]: A "destruction" (D) laser pulse at 800 nm excites a cold sample[13] into the disordered state, breaking up the CDW order. We then monitor the evolution of the transient reflectivity $\Delta R(t_{\text{DP}})/R$ excited with a weaker pump (P) pulse as a function of time delay t_{DP} between the D and P pulse (the pulse sequence nomenclature is illustrated in the insert to Fig. 1b)). The D pulse fluence is adjusted to twice the threshold for causing the destruction of the ordered state [5]. After a quench by the laser pulse, order recovers first through the sub-picosecond recovery of the quasiparticle gap leading to coherent oscillations of the OP and the coherent creation of TDs which decay within 5-8 ps in TbTe_3 [5]. Since the CDW coherence length (~ 2 nm) is much shorter than the size of the laser excited volume ($\sim 50 \mu\text{m}$ dia), order emerges with different phase in different regions, resulting in the formation of topological defects whose spatial distribution is determined partly by the inhomogeneous excitation and partly by the underlying fluctuations which nucleate the emergence of order by the so called Kibble-Zurek[2, 3] mechanism. The resulting inhomogeneity of the OP leads to observable temporally resolvable effects in the frequency, linewidth and amplitude of the collective amplitude mode, all of which are related to the OP, as shown in previous studies[7].

In Fig. 1(a) we show the raw data on the transient reflectivity $\Delta R(t_{\text{DP}})/R$ of TbTe_3 at different time delays t_{DP} after the D pulse. After the initial QP relaxation we observe oscillations due to the coherently excited order parameter amplitude mode (AM) and other phonons.[7–

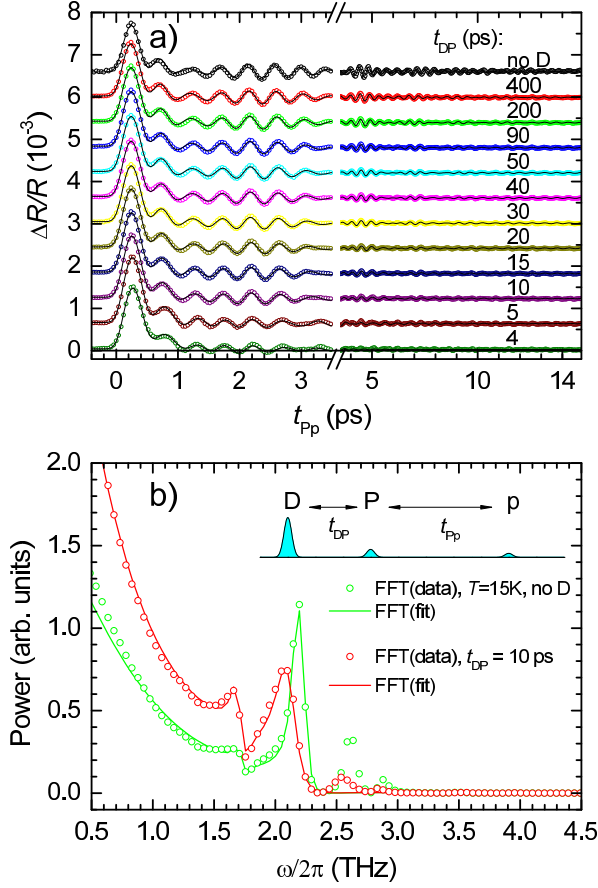


Figure 1: a) The transient reflectivity of TbTe₃ at different times t_{DP} after the D pulse. The thin lines are the fits discussed in text. b) An example of the FFT power spectra for the raw data and the fit at $t_{DP} = 10$ ps with and without a D pulse. The inset shows the laser pulse sequence.

9] The level of noise is very small, due to the the excellent intrinsic properties of the material, which helps us make a detailed quantitative analysis. We analyze the transient reflectivity oscillations using the theory for displacive excitation of coherent phonons:[10]

$$\begin{aligned} \frac{\Delta R(t_{PP})}{R} = & \int_0^\infty G(t-u) \times \\ & \times [A_e \exp(-u/\tau) + A_B] du \\ & + \sum A_i \int_0^\infty G(t-u) \exp(-\gamma_i u) \times \\ & \times [\cos(\Omega_i u) - \beta_i \sin(\Omega_i u)] du \quad (1) \end{aligned}$$

where $\beta_i = (1/\tau - \gamma_i)/\Omega_i$, $G(t) = \exp(-2t^2/\tau_P^2)$ and τ_P is the laser pulse length. The first integral represents the QP relaxation with the relaxation time τ , while the sum depicts the response of coherent phonons with frequencies Ω_i , and effective dampings γ_i . A_e corresponds to the QP relaxation amplitude while the residual value at long delays is A_B . To limit the number of fitting parameters we keep only two phonon terms corresponding to the AM

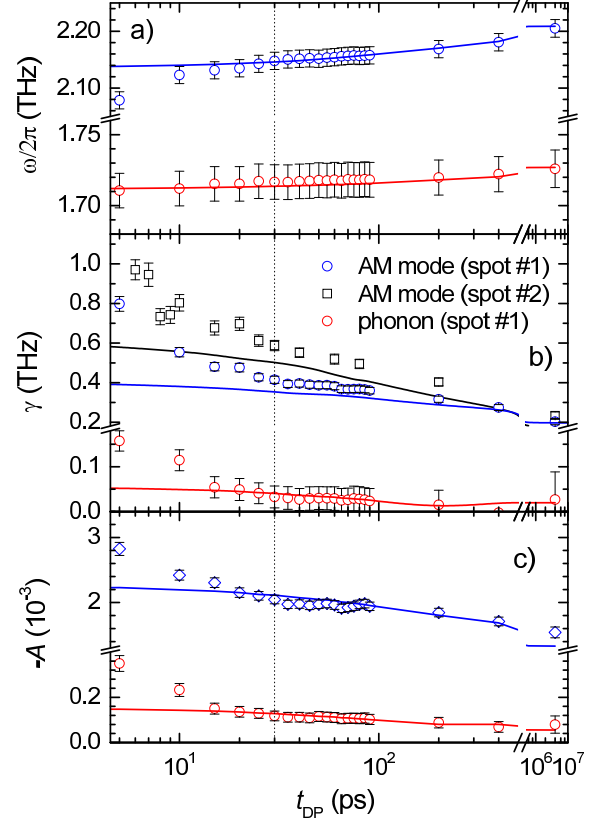


Figure 2: a) Frequencies of the AM and the 1.7-THz phonon as a function of t_{DP} . b) Effective dampings of the AM and the phonon as a function of t_{DP} . Open squares represent a measurement from another spot on the sample. c) Amplitudes of the AM and the phonon as a function of t_{DP} . The solid lines are the frequencies, linewidths and amplitudes calculated using an inhomogeneous temperature distribution model(Eq.2).

at 2.2 THz and the 1.7-THz phonon which strongly interacts with the AM at higher temperatures.[7] Fig 1(b) shows the fast Fourier transform (FFT) of the raw data and of the fit to the data i) without the D pulse and ii) for a D-P delay of $t_{DP} = 10$ ps, clearly showing that Eq. (1) fits the response very well below ~ 2.4 THz irrespective of t_{DP} .

The t_{DP} -dependence of the frequency, linewidth and amplitude of the AM and 1.7 THz phonon modes are shown in Fig. 2. The linewidth is shown for two sets of data obtained from different spots on the sample, showing an offset between the two data sets.

In order to obtain a calibration of the effective temperature T_{eff} of the photoexcited sample volume we measured *independently*, by means of a standard pump-probe experiment, the T -dependence of the reflectivity transients to determine the T -dependent amplitude, frequency $[\omega_{AM}(T)]$ and damping $[\gamma_{AM}(T)]$ for the AM. Us-

ing these calibrations we are in a position to determine T_{eff} as a function of time from $\omega_{\text{AM}}(t_{\text{DP}})$ and $\gamma_{\text{AM}}(t_{\text{DP}})$ and take it into account to obtain the thermal inhomogeneity dynamics. The time-dependence of the T_{eff} is shown in Fig. 3(b). We observe that the two effective temperatures $T_{\omega}(t_{\text{DP}})$ and $T_{\gamma}(t_{\text{DP}})$ obtained from the $\omega_{\text{AM}}(t_{\text{DP}})$ and $\gamma_{\text{AM}}(t_{\text{DP}})$ systematically differ by approximately 20 K. This difference arises because the order parameter is inhomogeneous within the probe volume, which increases the effective linewidth and consequently $T_{\gamma}(t_{\text{DP}})$. The order parameter inhomogeneity arises from both the *thermal inhomogeneity* and the presence of *topological defects*.

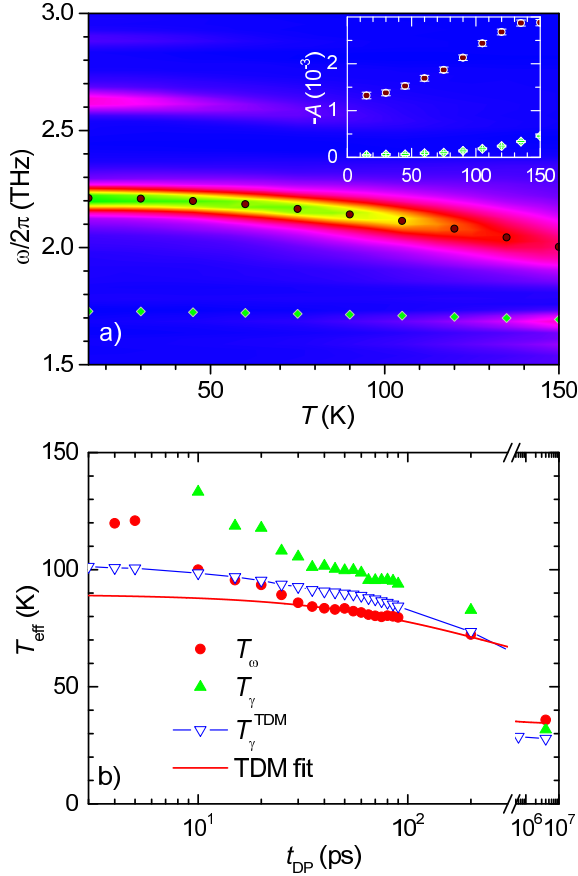


Figure 3: a) The temperature dependence of $\omega_{\text{AM}}(T)$ and $\gamma_{\text{AM}}(T)$ measured in a standard Pp experiment. The inset shows the T -dependence of the amplitudes for the AM (circles) and the 1.7-THz phonon (diamonds). b) The time-dependence of the effective temperature $T_{\text{eff}}(t_{\text{DP}})$ from $\omega_{\text{AM}}(t_{\text{DP}})$ and $\gamma_{\text{AM}}(t_{\text{DP}})$. The solid line is a fit to ω_{AM} using the thermal diffusion model. The inverted triangles correspond to the calculated $T_{\gamma}^{\text{TDM}}(t_{\text{DP}})$ taking into account the inhomogeneous temperature distribution given by Eq. (2).

To account for the thermal inhomogeneity we first fit a thermal diffusion model[11] (TDM) to the effective temperature from the AM frequency $T_{\omega}(t_{\text{DP}})$, and then use the TDM parameters to calculate the transient op-

tical response in the reflectivity which fully takes into account inhomogeneity of the temperature in the excited volume. As seen in Fig. 3 (b), $T_{\omega}(t_{\text{DP}})$ can be fit very well over 5 decades of time from 30 ps to 4 μs using a one-dimensional[14] TDM, where $T(t_{\text{DP}}) = \Delta T / \sqrt{1 + t_{\text{DP}}/\tau_D} + T_0$, and the fit parameter $\tau_D \sim 120$ ps represents the characteristic heat diffusion time[11].

Next we simulate the optical reflectivity response in the presence of the inhomogeneous temperature distribution using the thermal diffusion parameters obtained from the fit above. The response is given by:

$$\frac{\Delta R_{\text{TDM}}(t_{\text{DP}})}{R} \Big|_{t_{\text{DP}}} = \int_0^\infty e^{-3z/\lambda_{\text{op}}} \times \frac{\Delta R(t_{\text{DP}})}{R} \Big|_{T(z, t_{\text{DP}})} dz, \quad (2)$$

$$T(z, t_{\text{DP}}) = \Delta T \frac{e^{-z^2/[\lambda_{\text{op}}^2(1+t_{\text{DP}}/\tau_D)]}}{\sqrt{1 + t_{\text{DP}}/\tau_D}} + T_0. \quad (3)$$

where $\Delta R(t_{\text{DP}})/R|_{T(z, t_{\text{DP}})}$ in (2) is calculated by interpolation from the experimentally determined T -dependent transients and λ_{op} is the optical penetration depth. From the response in Eq. (2) we calculate the predicted thermally inhomogeneous linewidth $\gamma_{\text{AM}}^{\text{TDM}}(t_{\text{DP}})$, and other phonon parameters, as well as the effective temperature $T_{\gamma}^{\text{TDM}}(t_{\text{DP}})$ in the same way as previously using the temperature calibration data in Fig. 3 a).

Comparing now the simulation with the experiment in Fig. 2, we see that the validity of the TDM beyond ~ 30 ps is well supported by the good agreement of the simulation for both the AM and the 1.7-THz phonon parameters. We can thus safely conclude, that the recovery of the order parameter on timescales longer than ~ 30 ps is primarily governed by the 1D heat diffusion process.

Below ~ 30 ps however, there is a large discrepancy between the calculated T_{eff} , γ_{AM} and other phonon parameters in comparison to the data, even after carefully taking into account the thermal inhomogeneity. While the smaller spatially varying discrepancy for $\gamma_{\text{AM}}(t_{\text{DP}})$ [and $T_{\gamma}^{\text{TDM}}(t_{\text{DP}})$] at longer t_{DP} might possibly be attributed to a spatial variation of the intrinsic AM linewidth, [15] the observed magnitude and the evolution of $\gamma_{\text{AM}}(t_{\text{DP}})$ for $t_{\text{DP}} < 30$ ps clearly cannot be assigned solely to the temperature inhomogeneity. Subtracting the thermal contribution from the AM linewidth in Fig. 2 b), we can now isolate the contribution of the topological defects as shown in Fig. 4.

As discussed in the introduction some of the defects created in the quench process annihilate *coherently* resulting in an aperiodic modulation of the AM intensity and frequency in the first ~ 8 picoseconds[5]. The very low level of experimental noise in the raw data allows us to attribute the observed data scatter to the coherent defect dynamics in the material, rather than experimental noise.

The modulation of the AM due to the defects that annihilate *incoherently* is unfortunately not detected *di-*

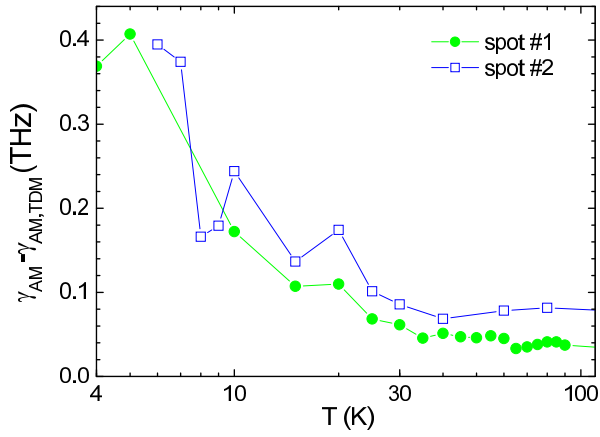


Figure 4: The time-dependence of γ_{AM} due to topological defect annihilation. Data for spot #1 and spot #2 on the sample show significant differences primarily in the long time behavior beyond 30 ps, which appears as an offset.

rectly by our stroboscopic technique. However, the incoherent topological defects give rise to a spatial inhomogeneity of the order parameter and a *decoherence* of the AM oscillations leading to an increased linewidth γ_{AM} for $t_{DP} < 30$ ps which we have detected in our experiments. Concurrently the defects give rise to a softening of the collective mode ω_{AM} , because of the OP suppression which they cause. The increase of the coupled 1.7-THz phonon effective damping at shorter t_{DP} as shown in Fig. 2 is presumably also caused by the inhomogeneity of the OP. A further manifestation of the incoherent annihilation is the increase of the amplitudes of the AM and the phonon with respect to the TDM for $t_{DP} < \sim 30$ ps, which is also consistent with the suppression of the OP when

one takes into account that the amplitudes of the modes increase with the decreasing OP amplitude deduced from their T -dependence shown in the inset of Fig. 3(a).

Apart from intrinsic topological defect annihilation processes, which we have identified on a timescale of 30 ps, we expect to observe annihilation of domain walls pinned to defects and imperfections at longer times. The timescale of their annihilation may extend well beyond 30 ps into microseconds. Evidence for such slower extrinsic recombination processes comes from the spot-to-spot variation shown in Figs. 2b) and 4. The dynamics on the shorter timescales up to 30 ps appears qualitatively the same in different spots, but the dynamics at longer timescales appears as a background which is strongly spot-dependent, as expected for pinned defect annihilation dominated by extrinsic sample imperfections or impurities.

In conclusion, these experiments demonstrate the possibility of studying both coherent and incoherent topological defects dynamics in complex materials in which the order parameter can be monitored in real time through the dynamics of the collective mode. The dynamics on a timescale of ~ 30 ps can unambiguously be associated with intrinsic topological defects annihilation in TbTe₃ following a laser quench arising from the time-dependent inhomogeneity and suppression of the order parameter. The inhomogeneity causes an increased effective damping of the amplitude mode while the suppression of the order-parameter is indicated by an additional softening of the AM-mode frequency. Beyond ~ 30 ps we find a predominantly thermal-diffusion governed order-parameter dynamics with a signature of extrinsic defect annihilation dynamics, suggested by significant variation from spot to spot across the sample.

-
- [1] Y. Bunkov and H. Godfrin, *Topological defects and the non-equilibrium dynamics of symmetry breaking phase transitions*, vol. 549 (Springer, 2000).
 - [2] T. W. B. Kibble, *Journal of Physics A: Mathematical and General* **9**, 1387 (1976), URL <http://stacks.iop.org/0305-4470/9/i=8/a=029>.
 - [3] W. Zurek, *Nature* **317**, 505 (1985).
 - [4] G. Grüner, *Density waves in solids* (Addison-Wesley New York, 1994).
 - [5] R. V. Yuzupov, T. Mertelj, P. Kusar, V. Kabanov, S. Brazovskii, J.-H. Chu, I. R. Fisher, and D. Mihailovic, *Nature Physics* **6**, 681 (2010).
 - [6] P. Kusar, T. Mertelj, V. V. Kabanov, J.-H. Chu, I. R. Fisher, H. Berger, L. Forró, and D. Mihailovic, *Phys. Rev. B* **83**, 035104 (2011), URL <http://link.aps.org/doi/10.1103/PhysRevB.83.035104>.
 - [7] R. V. Yuzupov, T. Mertelj, J.-H. Chu, I. R. Fisher, and D. Mihailovic, *Phys. Rev. Lett.* **101**, 246402 (2008), URL <http://link.aps.org/doi/10.1103/PhysRevLett.101.246402>.
 - [8] F. Schmitt, P. Kirchmann, U. Bovensiepen, R. Moore, L. Rettig, M. Krenz, J. Chu, N. Ru, L. Perfetti, D. Lu, et al., *Science* **321**, 1649 (2008).
 - [9] M. Lavagnini, H.-M. Eiter, L. Tassini, B. Muschler, R. Hackl, R. Monnier, J.-H. Chu, I. R. Fisher, and L. Degiorgi, *Phys. Rev. B* **81**, 081101 (2010), URL <http://link.aps.org/doi/10.1103/PhysRevB.81.081101>.
 - [10] H. J. Zeiger, J. Vidal, T. K. Cheng, E. P. Ippen, G. Dresselhaus, and M. S. Dresselhaus, *Phys. Rev. B* **45**, 768 (1992), URL <http://link.aps.org/doi/10.1103/PhysRevB.45.768>.
 - [11] T. Mertelj, A. Ošlak, J. Dolinšek, I. R. Fisher, V. V. Kabanov, and D. Mihailovic, *Phys. Rev. Lett.* **102**, 086405 (2009), URL <http://link.aps.org/doi/10.1103/PhysRevLett.102.086405>.
 - [12] N. Ru, C. Condon, G. Margulis, K. Shin, J. Laverock, S. Dugdale, M. Toney, and I. Fisher, *Physical Review B* **77**, 035114 (2008).
 - [13] The growth of the samples by a self-flux technique and subsequent characterization was described elsewhere.[12]
 - [14] The diameters of the beams are much larger than the optical penetration depth so on the relevant timescale the heat diffusion is 1D.
 - [15] In the standard 2-pulse pump-probe experiments we observe some spatial variation of the AM linewidth which

we assign to the intrinsic structural-defect/impurity density spatial variation in the sample. Although the care was taken that T -dependent standard 2-pulse Pp scans, used to obtain the data for simulation, were performed on the same spot on the sample (spot #1) as the 3-pulse DPp scans, some small daily drift of the spot position on the sample can not be excluded. A possible contri-

bution to the AM linewidth discrepancy at long t_{DP} by the spatial variation of the intrinsic AM linewidth is suggested by the larger discrepancy, observed beyond ~ 30 ps, between the data from another spot (spot #2) and the corresponding TDM simulation based on the first spot (spot#1) T -dependent scans [see Fig. 2 (b)].